JUL 1 7 1980 Hem 830-H-15 NAS 1.60: 1682
COMPLETED

NASA Technical Paper 1682

Effects of Various Assumptions on the Calculated Liquid Fraction in Isentropic Saturated Equilibrium Expansions

Joseph W. Bursik and Robert M. Hall

JUNE 1980

NASA

33

NASA Technical Paper 1682

Effects of Various Assumptions on the Calculated Liquid Fraction in Isentropic Saturated Equilibrium Expansions

Joseph W. Bursik
Rensselaer Polytechnic Institute
Troy, New York

Robert M. Hall
Langley Research Center
Hampton, Virginia

National Aeronautics
and Space Administration

Scientific and Technical
Information Office

1980

SUMMARY

The saturated equilibrium expansion approximation for two-phase flow often involves ideal-gas and latent-heat assumptions to simplify the solution procedure. This approach is well documented by Wegener and Mack and works best at low pressures approaching the triple point, for which deviations from ideal-gas behavior are small. A thermodynamic expression for liquid mass fraction that is decoupled from the equations of fluid mechanics is used in this paper to compare the effects of the various assumptions on nitrogen-gas saturated equilibrium expansion flow starting at 8.81 atm, 2.99 atm, and 0.45 atm, which are conditions representative of transonic cryogenic wind tunnels. For the highest-pressure case, the entire set of ideal-gas and latent-heat assumptions are shown to be in error by 62 percent for the values of heat capacity and latent heat used in this paper. This error appears to be chiefly the result of the inaccuracy of the ideal-gas expression for approximating entropy in nitrogen gas. An approximation of the exact, real-gas expression is also developed by using a constant, two-phase isentropic expansion coefficient which results in an error of only 2 percent for the high-pressure case.

INTRODUCTION

When condensation occurs in a wind tunnel, the resulting two-phase flow will usually cease to simulate the flow of an ideal diatomic gas, as explained in reference 1. Often it is of interest to be able to predict the approximate magnitude of these effects, and a useful analytic procedure to do this is to assume the flow undergoes a saturated equilibrium expansion in which the pressure and temperature of the two-phase mixture isentropically follow the vapor-pressure curve. Developed more fully in reference 1, this analytic procedure is only an idealization of actual condensing flow, although it does closely approximate the physical situation when there are many preexisting seed particles in the flow.

The saturated equilibrium expansion procedure can be solved exactly from a thermodynamic viewpoint, but it is usually solved approximately by using several thermodynamic assumptions which simplify the solution procedure to a large extent. The simplifying assumptions are described by Wegener and Mack in reference 1 and include representing the gas by the ideal-gas equations and treating latent heat as a constant. These assumptions are very adequate for the original application of the saturated equilibrium expansion procedure to hypersonic wind tunnels, where the flow usually becomes saturated at pressures one or two orders of magnitude below 1 atm. At low pressures, these approximations model the gas satisfactorily; however, as pressures increase, these assumptions will usually become more inaccurate.

A high-pressure application for the saturated equilibrium expansion problem has arisen with the development of nitrogen-gas, transonic cryogenic wind tunnels, which typically operate at reservoir pressures of 5 to 10 atm.

(See ref. 2.) Since under some test conditions the flow may become saturated at pressures of 5 atm or greater, an assessment of the accuracy of the ideal-gas approximations as used in the Wegener and Mack (ref. 1) development seems prudent for this higher pressure application.

Based on preliminary comparisons between the full (exact) thermodynamic analysis of nitrogen and the Wegener and Mack approach, it appears that the liquid mass fraction is the variable most sensitive to differences in approach. Consequently, a simple real-gas solution is developed and then manipulated to test the impact on predicted liquid mass fractions of the various assumptions either singly or in combination to give some understanding of the significance of the different assumptions that are involved in the Wegener and Mack development. A total of 12 approximate formulations are compared with the exact solutions for 3 different isentropes intersecting the nitrogen vapor-pressure curve at (120.0 K, 8.81 atm), (88.0 K, 2.99 atm), and (71.2 K, 0.45 atm). Of course, the complete set of assumptions used by Wegener and Mack is shown as one of the formulations. A particularly interesting comparison is found for an approximation that uses a constant two-phase isentropic expansion coefficient.

The section of this report entitled "Exact Models" contains a review of the necessary thermodynamics to derive the exact, real-gas expression for mass fraction of liquid and also contains details of the manipulation of the exact form into equivalent forms that will be used to derive the approximate expressions in the section "Approximate Models."

SYMBOLS

C_p heat capacity, J/kg·K

E generalized extensive two-phase property

e specific value of E, $\frac{E}{m}$

g liquid mass fraction, defined in equation (2)

ΔH latent heat, J/kg

h specific enthalpy, J/kg

k two-phase isentropic-expansion coefficient, defined in equation (15)

$\bar{k}_F$ assumed constant value of k fitted exactly at saturated-vapor and final states of an isentropic expansion

m mass, kg

p pressure, atm (1 atm = 101.3 kPa)

R nitrogen specific gas constant, J/kg·K

s specific entropy, J/kg·K

T temperature, K

v specific volume, m^3/kg

Subscripts:

c at point c, saturated-vapor state on an isentrope

F at point F, conditions at end of expansion

G at point G, saturated-vapor state

i index of model numbers, 0, 1, 2, . . ., 12

L at point L, saturated-liquid state

o at point o, reservoir conditions

p denotes conditions at constant pressure

r denotes reference conditions at a temperature 4 K below conditions at c

s denotes conditions at a constant entropy

Superscripts:

' denotes $\frac{d}{dT}$

- mean value

EXACT MODEL

An exact solution, or model, for liquid mass fraction is derived and manipulated into several equivalent exact forms. Before the exact model is derived, however, a review of the basic thermodynamics is given, starting with the sketches in figures 1 and 2.

Figure 1 illustrates, in a T,s diagram, an isentropic expansion $s = s_c$ emanating from a reservoir at T_o, p_o located in the one-phase superheat region. The isentrope contacts the boundary of the two-phase region at the point c where the liquid mass fraction g is zero. The expansion terminates at the final two-phase state F with $0 < g_F < 1$.

In figure 2, the entire two-phase region collapses into the single curve $p = p(T)$ which is the saturated vapor-pressure curve. This is true because the two-phase isotherms in s,T,p space are parallel straight lines which project as points in the p,T plane. Thus, the distinct two-phase points L, F,

and G of figure 1 project as the single point L,F,G of figure 2. Therefore, the isentrope ocF of figure 1 has two branches in figure 2, oc and cF, and the two-phase segment cF coincides with the vapor-pressure curve.

For a two-phase mixture of mass m a generalized, extensive-property symbol E may be used for any of the following: enthalpy, entropy, internal energy, Gibbs function, and Helmholtz function. The respective mixture specific values e = E/m are then obtained from

$$e(g,T) = e_G(T) - g[e_G(T) - e_L(T)] \tag{1}$$

This equation gives the specific value of any of the previously named extensive properties at any state defined by the pair of values g and T, provided the saturation values $e_L(T)$ and $e_G(T)$ are known at each temperature, as is usually the case. The liquid mass fraction g is defined for the two-phase region as

$$g = m_L/m \tag{2}$$

Therefore,

$$0 \leq g \leq 1 \tag{3}$$

As seen in figure 1, the saturated-vapor curve g = 0 is one branch of the boundary between the one-phase superheat region and the two-phase region. Similarly, the saturated-liquid curve g = 1 forms the other branch of the boundary which separates the one-phase liquid region from the two-phase region. The two branches of the boundary curves are joined smoothly at the critical point, from which other members of the constant g curves emanate into the two-phase region as sketched in the figure. All of the g = c family of curves collapse into the single vapor-pressure curve p = p(T) of figure 2.

In the condensing portion of the isentrope $s = s_c$, equation (1) can be used to give the liquid mass fraction by substituting s for e to give

$$g_0 = \frac{s_G - s_c}{s_G - s_L} \tag{4}$$

where the subscript 0 denotes any one of the equivalent exact forms. The subscript 0 also adds emphasis to the fact that no assumptions beyond the common one of constant entropy are used in the exact model.

A first equivalent form is obtained from equation (4) by adding and subtracting s_c in the denominator. This results in

$$g_0 = \frac{s_G - s_c}{s_G - s_c + s_c - s_L} \tag{5}$$

Even though only equivalent forms of the exact liquid mass fraction are derived in this section, it is nevertheless noted at this point that g_0 in equation (5) is now in a form in which the effect of the introduction of an ideal-gas entropy change for the saturated-vapor entropy difference $s_G - s_c$ is readily studied. In this case s_c would be obtained from appropriate thermodynamic tables at the arbitrarily fixed saturated-vapor state c and s_L would be read as the saturated-liquid value at successively lower temperatures from the same tables. In this way the effect of the single assumption could be isolated.

Additional exact forms of g_0 are obtained through the use of thermodynamic identities for the local latent heat $\Delta H(T)$. These are

$$\Delta H(T) = h_G(T) - h_L(T) \tag{6}$$

$$\Delta H(T) = T[s_G(T) - s_L(T)] \tag{7}$$

$$\Delta H(T) = Tp'(T)[v_G(T) - v_L(T)] \tag{8}$$

where $p'(T)$ is the slope of the vapor-pressure curve at temperature T. Equation (8) is known as the Clausius-Clapeyron equation. By equating the right sides of equations (7) and (8) and substituting for $s_G - s_L$ in equation (4), another equivalent form for the exact liquid mass fraction is given as

$$g_0 = \frac{s_G - s_c}{(v_G - v_L)p'} \tag{9}$$

The final equivalent form for g_0 comes from substituting equation (8) into equation (9) for $v_G - v_L$ to give

$$g_0 = \frac{T(s_G - s_c)}{\Delta H(T)} \tag{10}$$

For nitrogen, the right sides of all of the equivalent forms for g_0 (eqs. (4), (5), (9), and (10)) can be computed by using the saturation tables

found in reference 3. Of course, similar tables are available for computing these quantities for other gases as well.

APPROXIMATE MODELS

Different approximations can now be substituted into the exact expressions for g_0 to determine what influences the approximations have on the predicted mass fraction of condensed liquid. In all, 12 different approximate expressions are derived by using either one or more of the following assumptions: (1) the specific volume of the liquid is negligible compared to the specific volume of the gas, (2) the entropy of the gas can be approximated by that of an ideal gas, (3) the real gas can be represented by an ideal-gas equation of state, (4) the latent heat at a temperature T can be approximated by a value equal to the average of the latent heat at T and the latent heat at T_c, (5) the two-phase isentropic flow can be approximated by a two-phase, constant-valued expansion coefficient, and (6) the latent heat can be treated as a constant. The assumptions are summarized in table 1 for easy reference.

TABLE 1.- BASIC ASSUMPTIONS

Number	Assumption
1	$v_L \ll v_G$
2	$s_G - s_c = (s_G - s_c)_{\text{ideal gas}}$
3	$pv_G = RT$
4	$\overline{\Delta H}(T,T_c) = \frac{1}{2}[\Delta H(T) + \Delta H(T_c)]$
5	$k = \bar{k}_F$
6	$\Delta H = \text{Constant}$

The liquid mass fractions g calculated with these assumptions are designated by subscripts 1 to 12. The value of specific heat at constant pressure C_p used in the calculations is equal to the zero-pressure value of 1039 J/kg·K unless otherwise noted. The impact on the calculations for liquid mass fraction of using the value of C_p corresponding to finite pressure and low temperature is discussed in the appendix.

One-Assumption Models

For the one-assumption models the subscript of g corresponds to the numbered assumptions from table 1. Thus, the first one-assumption model for the liquid mass fraction is

$$g_1 = (s_G - s_c)/v_G p' \tag{11}$$

and is obtained by using assumption 1 with equation (9). After the approximation is made, all of the quantities in the right side are obtained from the vapor-pressure equation and the saturation tables of reference 3. This procedure will apply uniformly to all subsequent approximations also.

When assumption 2 is applied to equation (5), the result is

$$g_2 = \frac{C_p \ln \frac{T}{T_c} - R \ln \frac{p}{p_c}}{C_p \ln \frac{T}{T_c} - R \ln \frac{p}{p_c} + s_c - s_L} \tag{12}$$

Assumption 3 applied to equation (9) gives

$$g_3 = \frac{s_G - s_c}{\left(\frac{RT}{p} - v_L\right)p'} \tag{13}$$

In the next model the local latent heat $\Delta H(T)$ in equation (10) is arbitrarily replaced by its local arithmetic average $\overline{\Delta H}(T,T_c)$ to establish a degree of sensitivity to latent heat (assumption 4) on a one-assumption level before encountering subsequent integral situations for which the approximations require some form of averaging. Thus, equation (10) is simply replaced by

$$g_4 = \frac{T(s_G - s_c)}{\overline{\Delta H}(T,T_c)} \tag{14}$$

The last one-assumption model to be considered assumes a constant isentropic-expansion coefficient k. Although this model does not enter the development of the Wegener and Mack (ref. 1) procedure, it does present a simple alternate way to approach simplifying the expressions for liquid mass fraction. From the general definition of k,

$$k = -\frac{v}{p}\left(\frac{\partial p}{\partial v}\right)_s \tag{15}$$

Those thermodynamic states on an isentrope can be represented by the differential form

$$\frac{dp}{p} = -k \frac{dv}{v} \tag{16}$$

where k is variable. For some mean value $\bar{k}$, integration between p_c, v_c and the local coordinates p, v gives

$$v = v_c \left(\frac{p_c}{p} \right)^{1/\bar{k}} \tag{17}$$

or

$$\bar{k} = \frac{\ln \frac{p_c}{p}}{\ln \frac{v}{v_c}} \tag{18}$$

which shows that $\bar{k}$ is a local average which can vary as p and v vary on the isentrope. For a closed interval on the isentrope with end states of c and F, equation (18) yields a value of $\bar{k}$, now designated as $\bar{k}_F$, equal to

$$\bar{k}_F = \frac{\ln \frac{p_c}{p_F}}{\ln \frac{v_F}{v_c}} \tag{19}$$

For small variations in k, the local average $\bar{k}$ in equation (17) is replaced by $\bar{k}_F$ and consequently gives an approximation for the isentrope in the p, v plane as

$$v = v_c \left(\frac{p_c}{p} \right)^{1/\bar{k}_F} \tag{20}$$

This will satisfy the end states p_C, v_C and p_F, v_F exactly. After state c is specified by selecting T_C, state F is obtained as follows. Substitution of v for e in equation (1) results in

$$v = v_G - g(v_G - v_L) \tag{21}$$

which holds for any two-phase state. Elimination of g between this equation and equation (4) gives the specific volume on the isentrope as

$$v = v_G - \frac{s_G - s_C}{s_G - s_L}(v_G - v_L) \tag{22}$$

In this equation s_C is the entropy of the saturated vapor which is fixed by the selection of T_C. All of the remaining quantities are saturation quantities which can be treated as functions of temperature; hence

$$v_F = v_G - \frac{s_G - s_C}{s_C - s_L}(v_G - v_L) \tag{23}$$

where equation (23) is evaluated at T_F. The definition of $\bar{k}_F$ in equation (19) is completed by taking p_F as the pressure on the vapor-pressure curve at T_F.

After eliminating v from equations (20) and (21), the result is rearranged to give the approximate model for the liquid mass fraction as

$$g_5 = \frac{v_G - v_C\left(\frac{p_C}{p}\right)^{1/\bar{k}_F}}{v_G - v_L} \tag{24}$$

In this equation v_g, v_L, and p are read from the thermodynamic tables at any temperature.

Two-Assumption Models

The two-assumption models are derived by adding an additional assumption to some of the one-assumption models. With more than one assumption occurring within a model, it is no longer possible to have the subscript on g simultaneously identify both the model number and the assumption number. Hence, the

notation is extended by writing the assumption numbers in parentheses after g_i, where i is the model number. Imposing the additional assumption 3 on equation (11) gives

$$g_6(1,3) = \frac{p(s_G - s_C)}{p'RT} \tag{25}$$

That is, the two-assumption model g_6 is constructed by using assumptions 1 and 3 from table 1. When assumption 2 is incorporated into equation (11), the result is

$$g_7(1,2) = \frac{C_p \ln \frac{T}{T_C} - R \ln \frac{p}{p_C}}{p'v_G} \tag{26}$$

Equation (13) with assumption 2 is

$$g_8(3,2) = \frac{C_p \ln \frac{T}{T_C} - R \ln \frac{p}{p_C}}{\left(\frac{RT}{p} - v_L\right)p'} \tag{27}$$

Finally, the combination of assumption 2 and equation (14) yields

$$g_9(4,2) = \frac{T\left(C_p \ln \frac{T}{T_C} - R \ln \frac{p}{p_C}\right)}{\overline{\Delta H}(T,T_C)} \tag{28}$$

Multiple-Assumption Models

A three-assumption model is obtained when assumption 3 is added to equation (26) to give

$$g_{10}(1,2,3) = \frac{p\left(C_p \ln \frac{T}{T_c} - R \ln \frac{p}{p_c}\right)}{RTp'} \tag{29}$$

The same result can be obtained by adding assumption 2 to equation (25), or by adding assumption 1 to equation (27). At this point it is again noted that the right sides of all g_i for $i = 0, 1, \ldots, 10$ are computed from Jacobsen's tables of thermodynamic properties (ref. 3). This means that p and p' are the actual values of the pressure and its derivative along the vapor-pressure curve. A new approximation is now incorporated for the vapor-pressure curve that necessitates the introduction of the local average latent heat in a formal way in, contrast to the arbitrary manner in which it was previously used. From equation (8) and assumptions 1 and 3,

$$\frac{p'}{p} = \frac{\Delta H(T)}{RT^2} \tag{30}$$

Next, the law of the mean can be used when integrating the right side of equation (30) to remove an exact mean value of latent heat $\langle \Delta H(T) \rangle$ from the integral. This mean value can then be approximated by $\overline{\Delta H}(T,T_c)$ of assumption 4. Consequently, by approximating this mean value with assumption 4, integration of equation (30) results in

$$-R \ln \frac{p}{p_c} = \overline{\Delta H}(T,T_c)\left(\frac{1}{T} - \frac{1}{T_c}\right) \tag{31}$$

The local average latent heat will again be referred to as assumption 4. Therefore,

$$g_{11}(1,2,3,4) = \frac{C_p T}{\Delta H(T)} \ln \frac{T}{T_c} + \frac{\overline{\Delta H}(T,T_c)}{\Delta H(T)}\left(1 - \frac{T}{T_c}\right) \tag{32}$$

where $\Delta H(T)$ is the actual local value of latent heat and $\overline{\Delta H}(T,T_c)$ is defined by assumption 4.

Finally, incorporating assumption 6 into equation (32), no distinction is made in the various latent heats. That is, only one value of latent heat,

$$\Delta H \sim \Delta H(T) \sim \overline{\Delta H}(T,T_c) \tag{33}$$

is used. With this, equation (32) reduces to equation (4.60) of reference 1, which has been previously referred to as the Wegener and Mack model. Therefore,

$$g_{12} = \frac{C_p T}{\Delta H} \ln \frac{T}{T_c} + \left(1 - \frac{T}{T_c}\right) \tag{34}$$

In reference 1, this has been derived from a fluid mechanics approach rather than the thermodynamics approach used here. The present approach emphasizes the fact that the liquid-mass-fraction calculation can be decoupled from the fluid mechanics. The thermodynamic state, which includes g, is the same at some temperature T (less than T_c) for two different superheat-reservoir choices on the same isentrope even though the velocities at temperature T are different for the two choices.

It is interesting to note that equation (34) uses the maximum number of assumptions and minimizes dependence on tables of thermodynamic properties. For example, C_p was normally taken to be the ideal-gas value of 1039 J/kg·K and, after arbitrarily selecting T_c and T_F, latent heat was taken to be

$$\Delta H = \frac{1}{2}[\Delta H(T_c) + \Delta H(T_F)] \tag{35}$$

and calculated from the tables in reference 3. Once these numbers are inserted into equation (34), g_{12} becomes an explicit, simple function of temperature.

RESULTS AND DISCUSSION

The computational results for the liquid mass fractions associated with three saturated equilibrium expansions for nitrogen are shown in figures 3 to 11. Figures 3 to 5 refer to an isentropic expansion from T_c = 102.0 K and p_c = 8.81 atm to T_F = 94.8 K and p_F = 5.26 atm. The next expansion is shown in figures 6 to 8 with T_c = 88.0 K, p_c = 2.99 atm, T_F = 80.8 K, and p_F = 1.47 atm. The final expansion corresponds to figures 9 to 11 with T_c = 71.2 K, p_c = 0.45 atm, T_F = 64.0 K, and p_F = 0.14 atm. For reference, the critical and triple-point temperatures are 126.2 K and 63.1 K, respectively. For any one expansion, each figure contains the zero-assumption model plotted as g_0. In addition, the first figure in each expansion shows the plots of the one-assumption models; the second figure shows the two-assumption models; and the third figure shows the multiple-assumption models.

For figures 3 to 11 all of the curves intersect at the point $T = T_c$ and $g = 0$, and generally they form an approximately linear pencil of curves emanating from the point of intersection. With the exception of the $\bar{k}_F$ curve (model 5), the curves do not intersect after the common $(T_c, 0)$ point, and like-numbered curves maintain the same relative position for each of the three

isentropic expansions. The overall width of the pencil fan measured at the respective T_F values is broadest for the high-temperature and high-pressure expansion, decreases for the midrange temperature and pressure expansion, and is the narrowest for the low-temperature and low-pressure expansion. The decreasing fan width associated with decreasing T_c values reflects the general fact that the imposed assumptions 1, 2, 3, 4, and 6 are all more accurate at low temperatures and pressures away from the critical point. The exception to this is the $\bar{k}_F$ curve (assumption 5), which has its poorest performance in the low-temperature expansion and its best performance in the middle-temperature expansion. (Assumption 5 is developed as an approximation of real-gas thermodynamics in contrast to the other assumptions that are generally of an ideal-gas, or zero-pressure, nature.)

The percent deviations of the predicted values of g from the exact model are presented in table 2 for each approximate model. The reference temperature

TABLE 2.- PERCENT DEVIATIONS OF APPROXIMATE LIQUID MASS FRACTIONS g_i FROM EXACT LIQUID MASS FRACTION g_0

Model	Percent deviation of g_i from g_0 for T_r of - (a)		
	98.0 K	84.0 K	67.2 K
1	-4.49(3)	-1.48(6)	0.00(9)
2	-35.09(3)	-16.02(6)	-3.82(9)
3	-17.15(3)	-7.42(6)	-1.53(9)
4	2.64(3)	1.78(6)	1.27(9)
5	1.85(3)	-.30(6)	-4.33(9)
6	-19.79(4)	-8.31(7)	-1.53(10)
7	-38.79(4)	-17.80(7)	-4.07(10)
8	-46.97(4)	-22.85(7)	-5.60(10)
9	-34.30(4)	-15.13(7)	-2.80(10)
10	-48.81(5)	-23.44(8)	-5.60(11)
11	-64.38(5)	-30.86(8)	-7.38(11)
12	-62.27(5)	-29.08(8)	-5.85(11)

[a]Numbers in parentheses refer to figure numbers.

T_r for each of the isentropes is 4 K below the value of T_c. The reason for choosing a temperature located approximately halfway between T_c and T_F for any run is that the $\bar{k}_F$ curve is constructed to produce no deviation at the end states. Its maximum error occurs at some temperature between T_c and T_F, which is roughly approximated by T_r. There are three values of T_r listed in table 2, one for each set of values for T_c and T_F. The percent deviation is defined as $100(g_i - g_0)/g_0$. For quick reference to the curves, the model num-

ber is given in the first column and the appropriate figure number is given in parentheses after the deviation.

The performance of the different assumptions is indicated in table 2. As expected, their performance at the high-pressure expansion (T_r = 98.0 K) is generally the poorest. Of the one-assumption models (models 1 to 5) the worst performance is by model 2 and the next to the worst is by model 3. Model 2 is the assumption that the entropy of gaseous nitrogen can be represented by an ideal-gas model and model 3 is the assumption that gaseous nitrogen can be represented by an ideal equation of state. Of the two-assumption models (models 6 to 9), all incorporate the entropy assumption and show poor performance. The poorest of these, model 8, incorporates both the entropy and the ideal equation of state assumptions. Of the multiple-assumption models, all perform poorly and all incorporate the ideal form of the entropy assumption. The entropy assumption seems to consistently be an inaccurate assumption that leads to errors, and the reasons for its inaccuracies are discussed in the appendix.

With the exception of model 5, the performance of the models improves markedly at the lower temperature and pressure expansions. Model 12, which corresponds to the assumptions in the Wegener and Mack procedure (ref. 1), departs from the exact model g_0 by about -62, -29, and -6 percent for the expansions starting at 8.81, 2.99, and 0.45 atm, respectively. At the lowest-pressure case model 12 does satisfactorily, which is good performance considering its original application was for much lower pressures for which agreement would be even better. It is recommended that model 12 not be used in cryogenic-nitrogen wind tunnels if saturation is expected at pressures over 0.5 atm and accuracy is required.

For application to other test gases it is recommended to repeat the procedure described herein to examine the various assumptions and their performance in predicting liquid mass fractions. An additional concern with other test gases is that the liquid mass fraction may not necessarily be the most sensitive difference between an exact solution and a procedure such as that of Wegener and Mack. For example, differences in liquid mass fraction may be less than differences in static pressure or temperature ratios at a given Mach number in other gases. Thus, the sensitivity to liquid mass fraction should be verified before relying solely on the liquid mass fraction test to determine whether or not the ideal approximations of Wegener and Mack can adequately describe the saturated equilibrium expansion problem.

CONCLUSIONS

The isentropic two-phase saturated equilibrium expansion problem is usually solved by using several simplifying approximations dealing with either ideal-gas or latent-heat assumptions, as in the formulation of Wegener and Mack (ref. 1). These assumptions are intended for low-pressure applications and begin to break down for the prediction of liquid mass fraction as the pressure at which the isentrope meets the vapor-pressure curve increases. For intersection pressures of 0.45, 2.99, and 8.81 atm in nitrogen, the differences between the exact, real-gas value of liquid mass fraction and the value predicted by the Wegener

and Mack formulation are, respectively, about -6, -29, and -62 percent. The assumption in the Wegener and Mack formulation that appears to generate the largest deviations for nitrogen is that of assuming the ideal-gas form for entropy of the gas phase. For nitrogen gas it is recommended that the Wegener and Mack formulation for solving saturated equilibrium expansions be restricted to pressures less than 0.5 atm. For pressures greater than 0.5 atm, either a full real-gas analysis or a procedure such as that with a constant isentropic-expansion coefficient should be used.

Langley Research Center
National Aeronautics and Space Administration
Hampton, VA 23665
April 23, 1980

APPENDIX

DISCUSSION OF THE IDEAL-GAS ENTROPY ASSUMPTION FOR NITROGEN

Attention was first directed to the assumption of the ideal-gas form of entropy after an attempt was made to improve the agreement between the multiple-assumption models (numbers 10 to 12) and the exact model g_0 for the high-pressure example shown in figure 5. Since all the calculations used in the approximate models in table 2 and figures 3 to 11 used the zero-pressure, ideal value of C_p (1039 J/kg·K), it was thought that using an average of the actual values of C_p along the expansion would lead to better agreement between g_0 and models 10, 11, and 12. As seen in figure 12, this did not occur. The agreement is noticeably worse with the more accurate value of C_p than with the zero-pressure value used in figure 5. As it has turned out, the problem is not just with C_p but with the entire ideal-gas approximation for $s_{G,F} - s_c$. (In this appendix the notation $s_{G,F}$ is used to denote the saturated-vapor entropy at the temperature $T_F = 94.8$ K. The use of the single subscript G is retained for variable saturated-vapor states.)

Consider the following methods for calculating the saturated-vapor entropy difference $s_{G,F} - s_c$ for the high-temperature expansion from $T_c = 102.0$ K to $T_F = 94.8$ K. Since both states in the entropy difference are single-phase gas states, the general expression for ds can be written without any assumptions as

$$ds = C_{p,G}\frac{dT}{T} - p\left(\frac{\partial v}{\partial T}\right)_{p,G}\frac{dp}{p} \tag{36}$$

Integration from c to the saturated-vapor state at T_F along the saturated-vapor curve gives

$$s_{G,F} - s_c = \langle C_{p,G}\rangle \ln\frac{T_F}{T_c} - \left\langle p\left(\frac{\partial v}{\partial T}\right)_{p,G}\right\rangle \ln\frac{p_F}{p_c} \tag{37}$$

Equation (37) is exact when the bracketed terms represent the value of the terms from the mean-value integral theorem of calculus. An arbitrary approximation or averaging for the bracketed terms can lead to deviations in the resulting entropy calculations. Several methods of computing the entropy difference, including the exact method, are now utilized to illustrate the effect of various approximations.

First, by assuming the ideal-gas equation of state $pv = RT$, then $p(\partial v/\partial T)_{p,G} = R$. Substitution into equation (37) results in

APPENDIX

$$(s_{G,F} - s_c)_{\text{ideal gas}} = \langle C_{p,G} \rangle \ln \frac{T_F}{T_c} - R \ln \frac{p_F}{p_c} \tag{38}$$

This form still leaves open the manner of approximating $\langle C_{p,G} \rangle$. Ordinarily the zero-pressure value of $C_{p,G}$ is incorporated with the ideal-gas concept. This value varies slowly in the present temperature range with an excellent approximation given by the value of 1039 J/kg·K, which is the value used in figures 3 to 11. The arithmetic mean of $C_{p,G}$ at saturated pressures, given by $[C_{p,G}(T_c) + C_{p,G}(T_F)]/2$, has the value 1418 J/kg·K and is used in the curves of figure 12. These figures indicate that both the ideal and arithmetic-mean values of $C_{p,G}$ in conjunction with equations (38) and (5) underestimate the liquid mass fraction with the arithmetic mean of the actual values at pressure, giving worse results. Specifically in terms of entropy differences, the exact solution calculates $s_{G,F} - s_c$ as equal to 115.8 J/kg·K for the high-temperature expansion, equation (38) with the ideal values of $C_{p,G}$ calculates $s_{G,F} - s_c$ as 77.1 J/kg·K and equation (38) with the arithmetic-mean values of C_p calculates $s_{G,F} - s_c$ as 49.3 J/kg·K.

Consequently, correcting $C_{p,G}$ to a more accurate value in equation (38) leads to worse agreement and this draws attention back to equations (37) and (38). In going from equation (37) to equation (38), the substitution involved assumes an ideal-gas equation of state to calculate $p(\partial v/\partial T)_{p,G} = R$, where $R = 296.8$ J/kg·K. This substitution actually represents a large source of error because the arithmetic-mean value of $p(\partial v/\partial T)_{p,G}$ evaluated at the end points of the high-temperature expansion is actually 431.2 J/kg·K. In fact, calculating $s_{G,F} - s_c$ from equation (37) with the arithmetic-mean values of both $C_{p,G}$ and $p(\partial v/\partial T)_{p,G}$ leads to a good value of 118.6 J/kg·K compared to the actual value of 115.8 J/kg·K, and would lead to excellent agreement for the predicted values of liquid mass fraction.

From this analysis, both bracketed terms in equation (37) are very important. In fact it is the $p(\partial v/\partial T)_{p,G}$ term that makes the ideal-gas entropy equation inaccurate in representing real-nitrogen values of entropy. This inaccuracy appears to be the primary reason why the equations in the analyses for liquid mass fraction using the ideal expression for entropy did so poorly.

REFERENCES

1. Wegener, P. P.; and Mack, L. M.: Condensation in Supersonic and Hypersonic Wind Tunnels. Advances in Applied Mechanics. Volume V, H. L. Dryden and Th. von Karman, eds., Academic Press, Inc., 1958, pp. 307-447.

2. Kilgore, Robert A.; Igoe, William B.; Adcock, Jerry B.; Hall, Robert M.; and Johnson, Charles B.: Full-Scale Aircraft Simulation With Cryogenic Tunnels and Status of the National Transonic Facility. NASA TM-80085, 1979.

3. Jacobsen, Richard T.: The Thermodynamic Properties of Nitrogen From 65 to 2000 K With Pressures to 10,000 Atmospheres. Ph. D. Thesis, Washington State Univ., 1972. (Available as NASA CR-128526.)

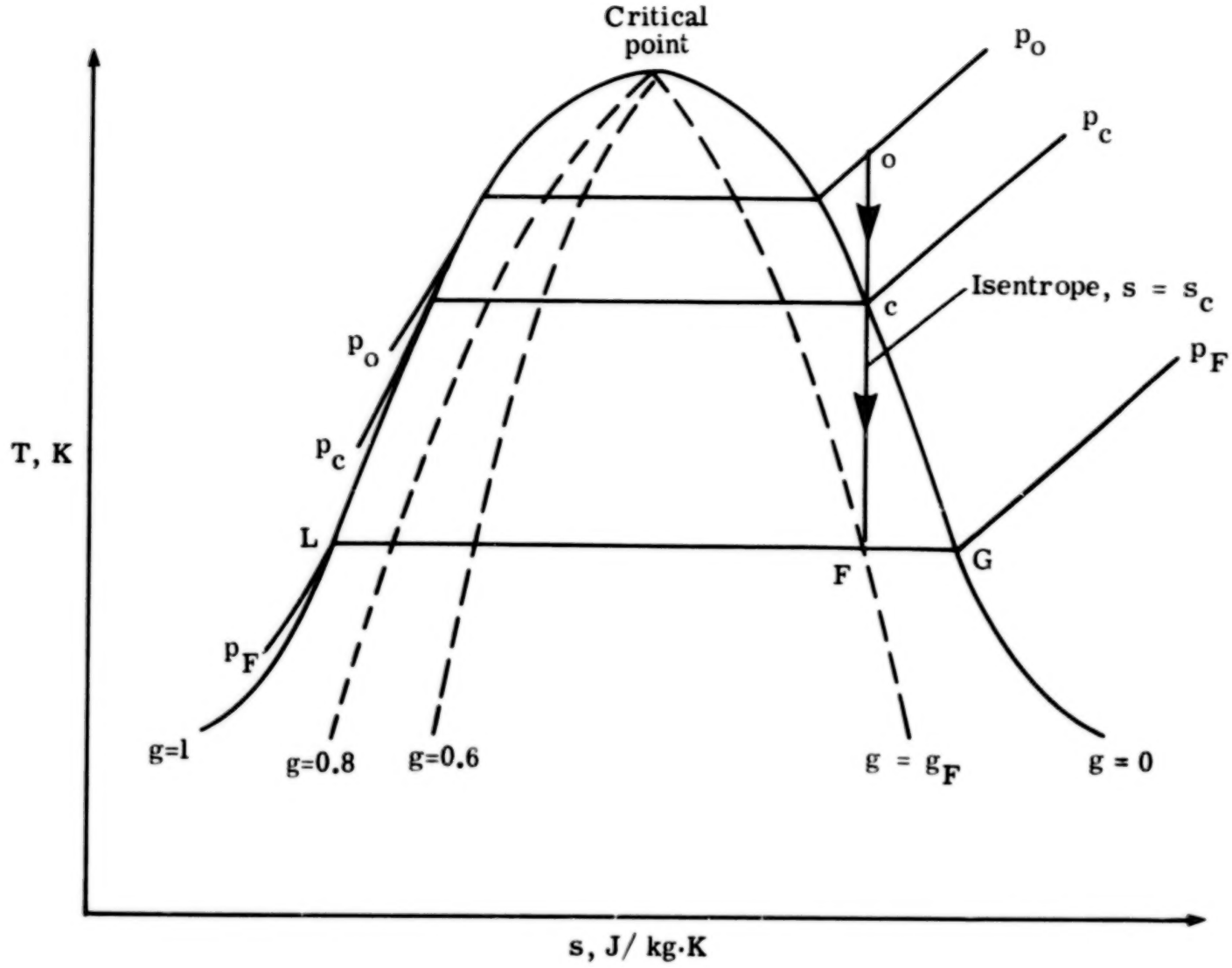

Figure 1.- Isentropic expansion in T,s diagram.

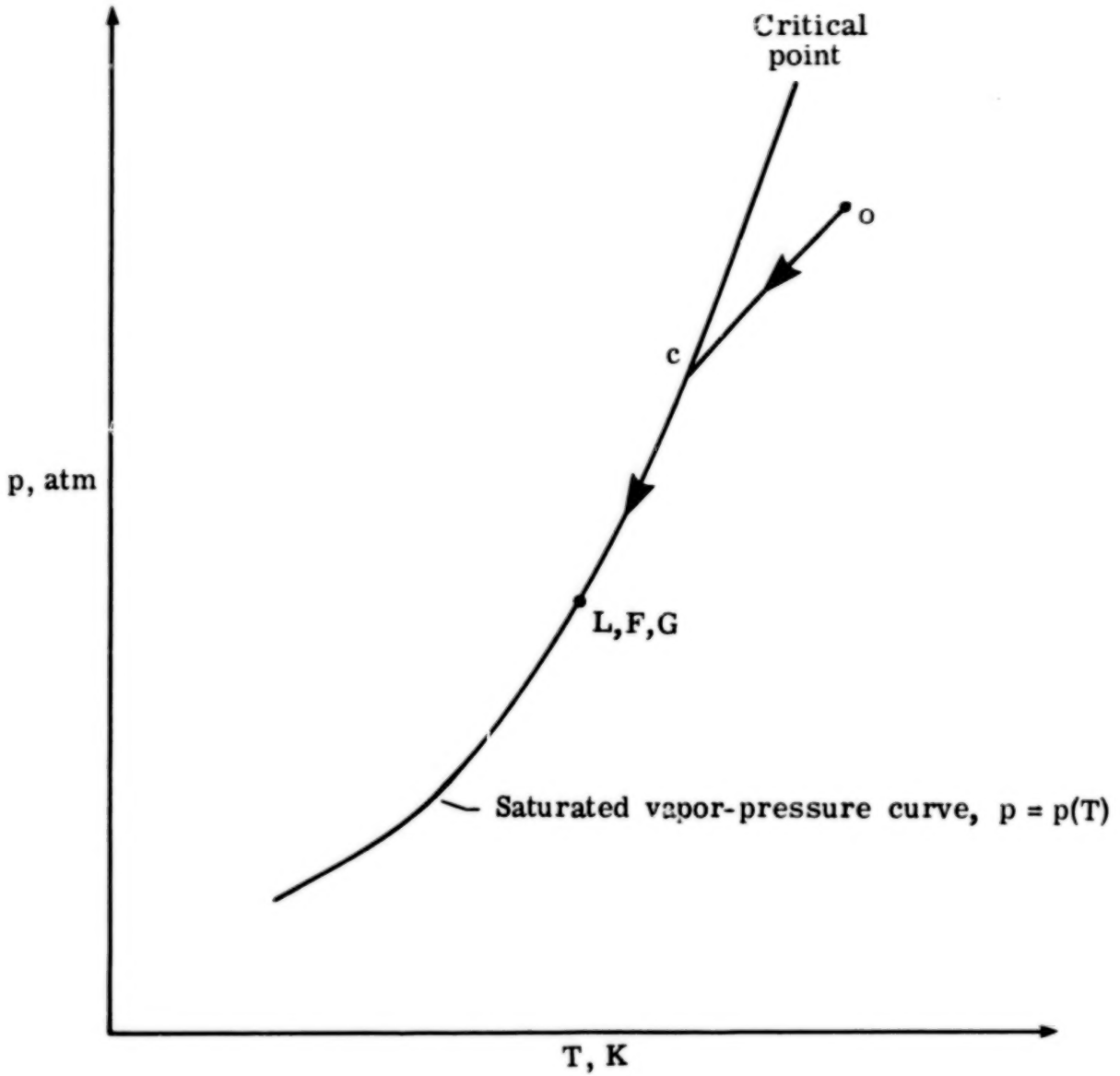

Figure 2.- Transformation of the isentropic expansion.

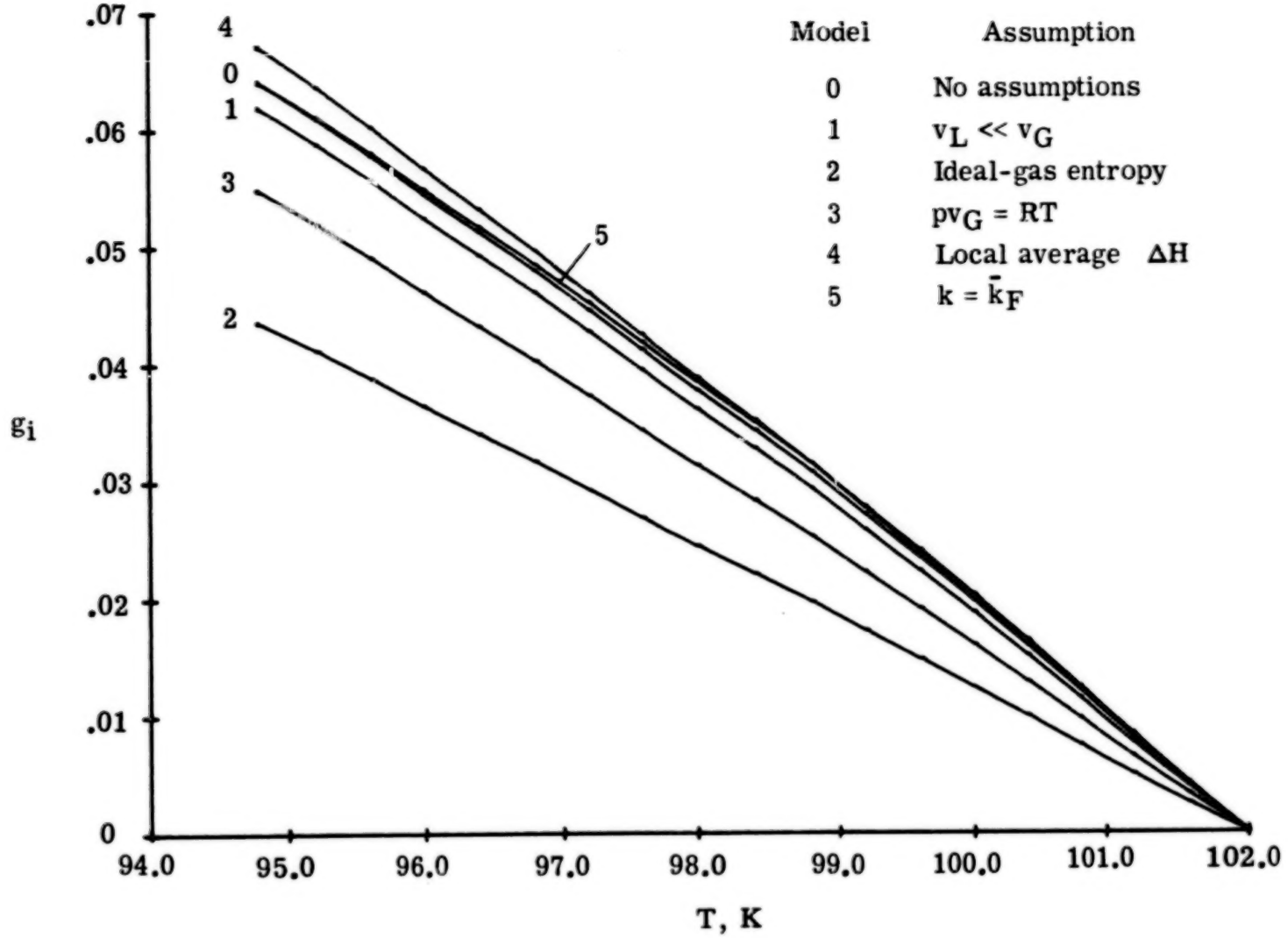

Figure 3.- Isentropic liquid mass fractions g_i for no-assumption and one-assumption models. T_C = 102.0 K; p_C = 8.81 atm; T_F = 94.8 K; p_F = 5.26 atm.

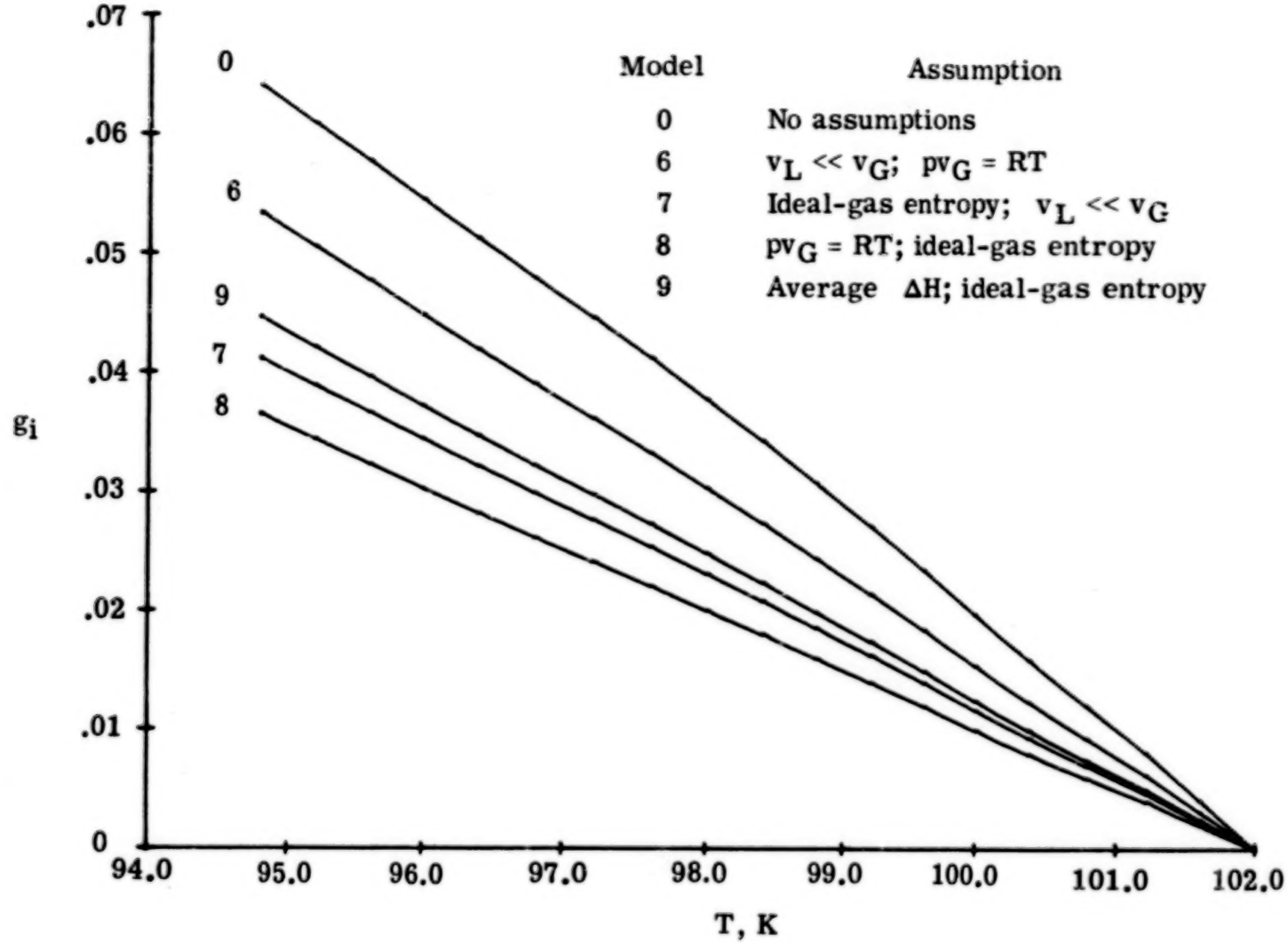

Figure 4.- Isentropic liquid mass fractions g_i for no-assumption and two-assumption models. T_C = 102.0 K; p_C = 8.81 atm; T_F = 94.8 K; p_F = 5.26 atm.

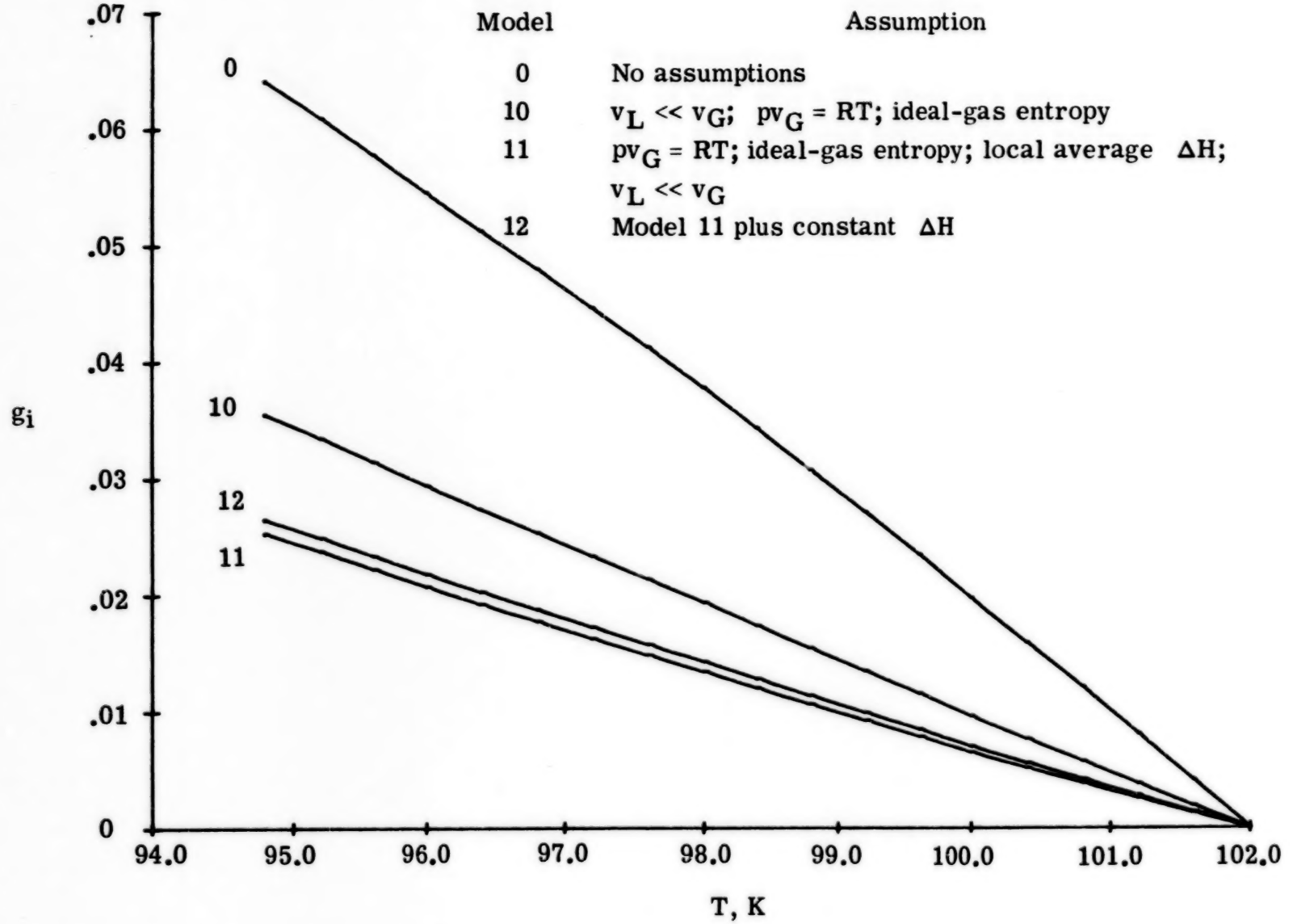

Figure 5.- Isentropic liquid mass fractions g_i for no-assumption and multiple-assumption models. T_C = 102.0 K; p_C = 8.81 atm; T_F = 94.8 K; p_F = 5.26 atm.

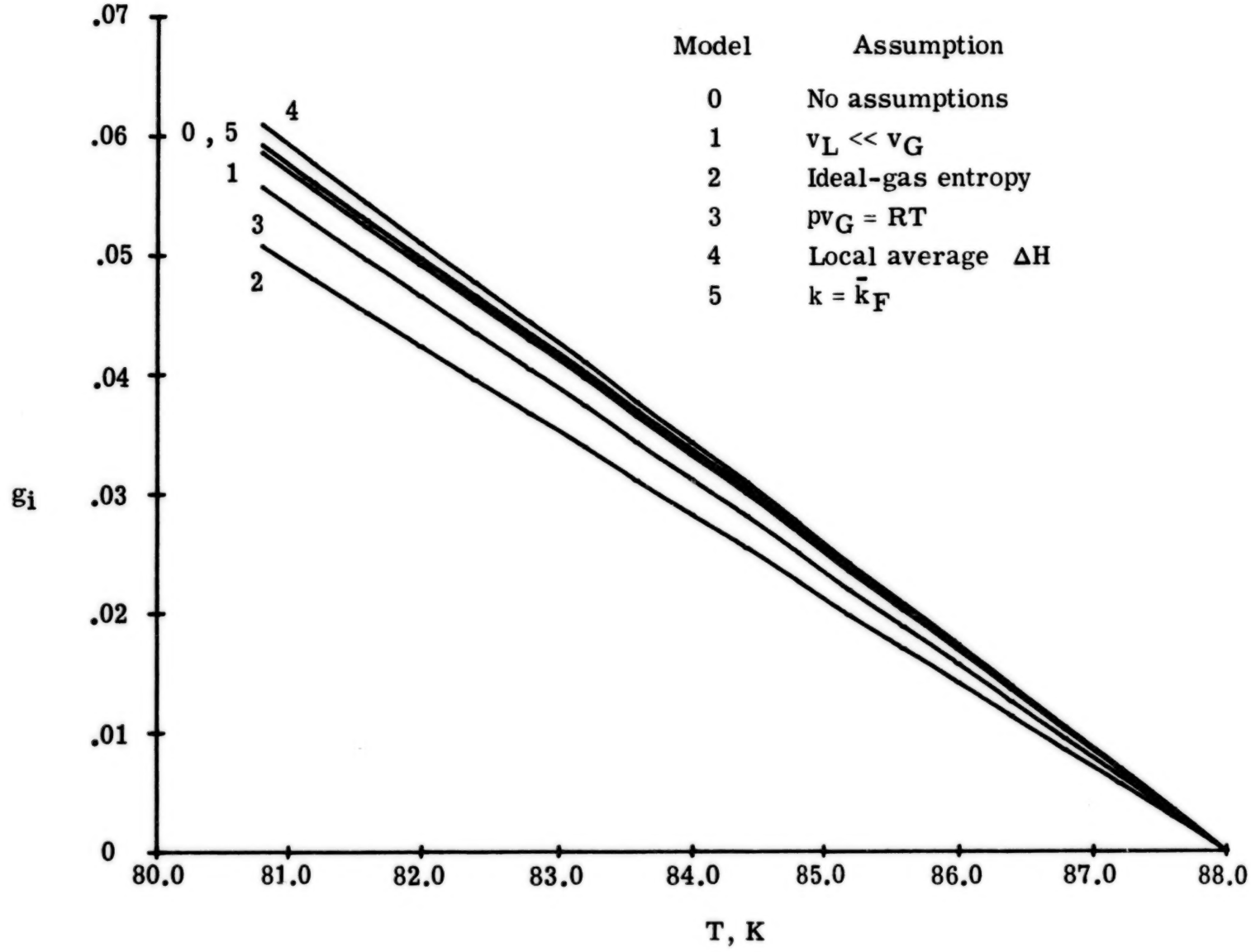

Figure 6.- Isentropic liquid mass fractions g_i for no-assumption and one-assumption models. T_C = 88.0 K; p_C = 2.99 atm; T_F = 80.8 K; p_F = 1.47 atm.

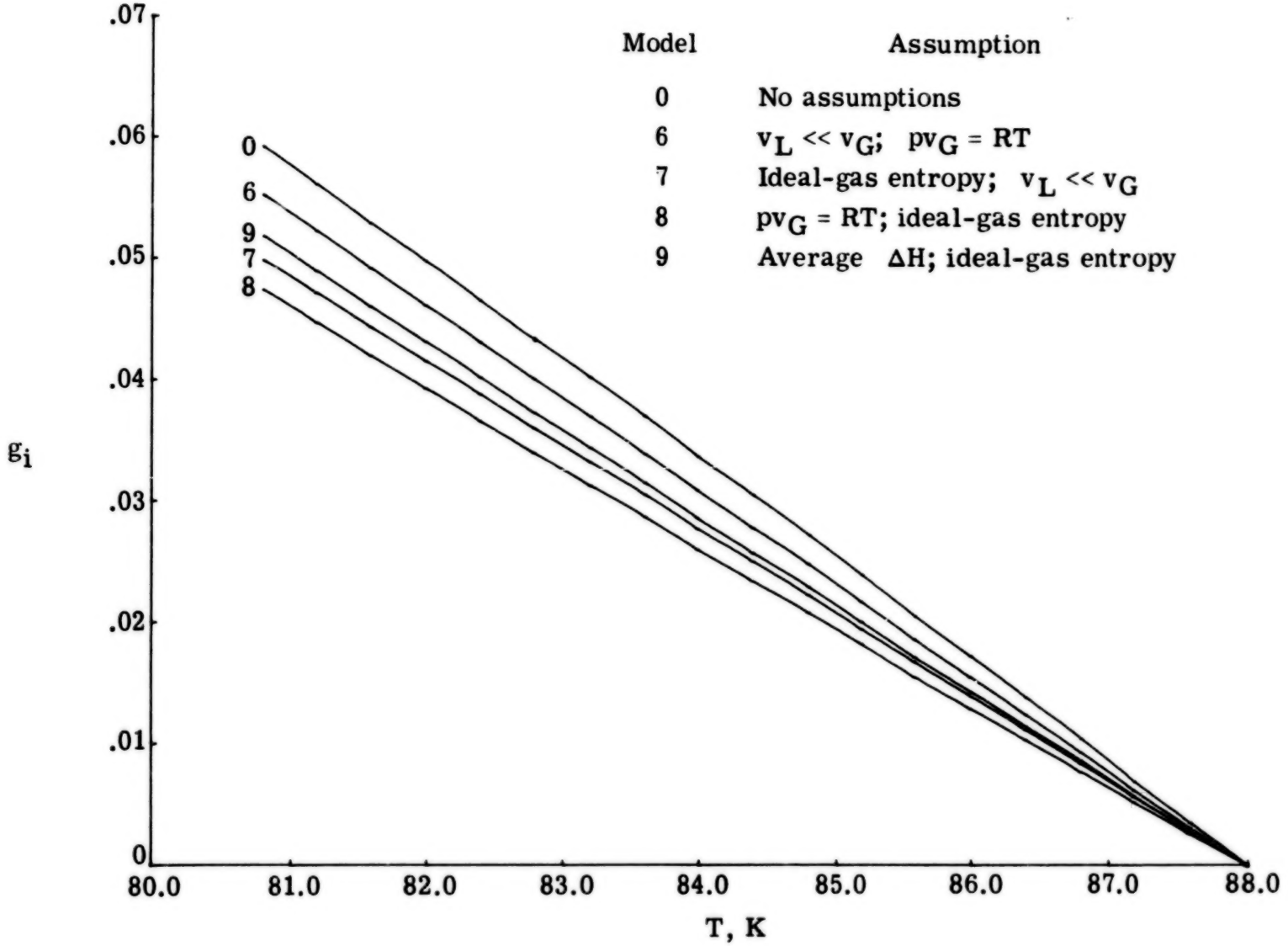

Figure 7.- Isentropic liquid mass fractions g_i for no-assumption and two-assumption models. T_c = 88.0 K; p_c = 2.99 atm; T_F = 80.8 K; p_F = 1.47 atm.

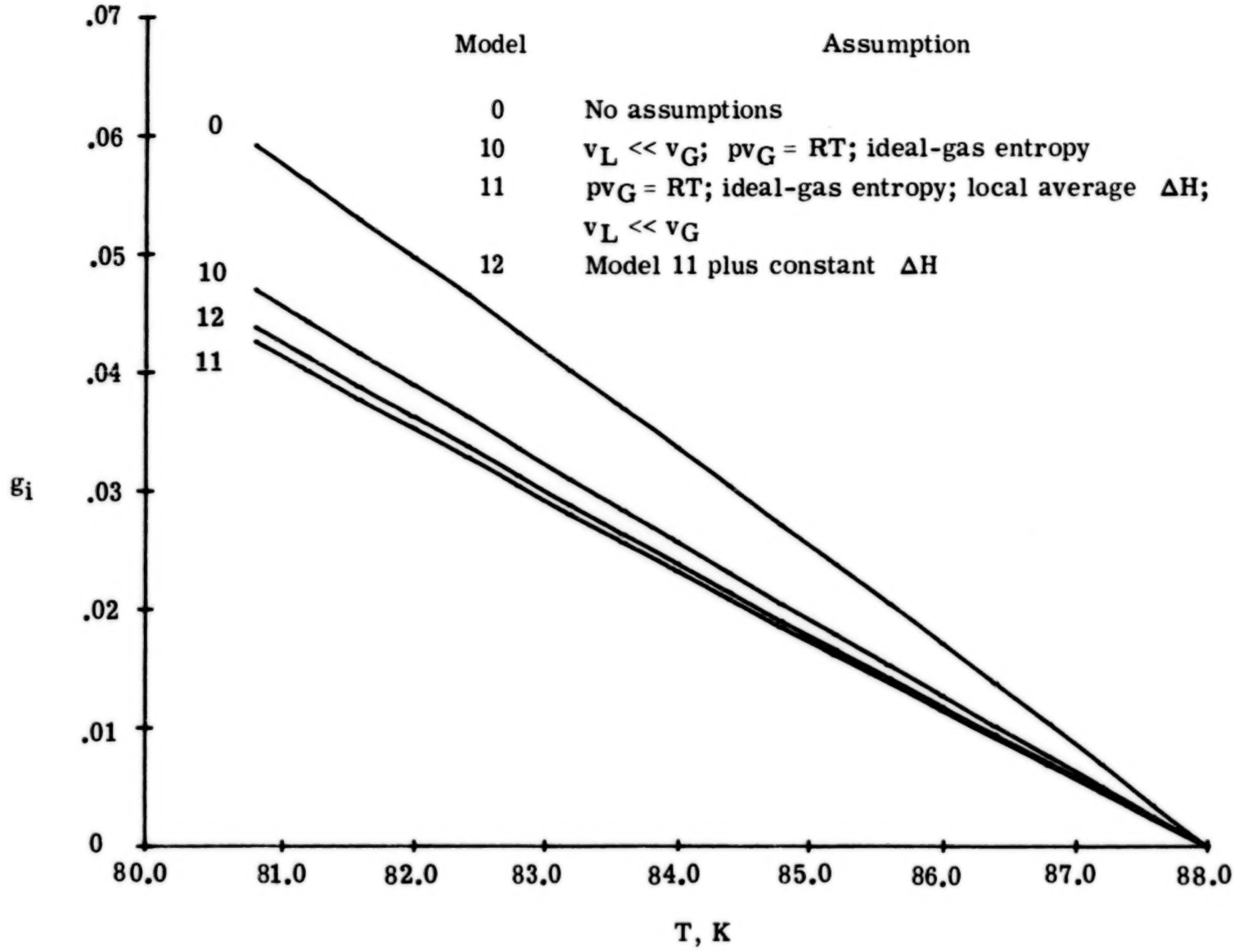

Figure 8.- Isentropic liquid mass fractions g_i for no-assumption and multiple-assumption models. T_C = 88.0 K; p_C = 2.99 atm; T_F = 80.8 K; p_F = 1.47 atm.

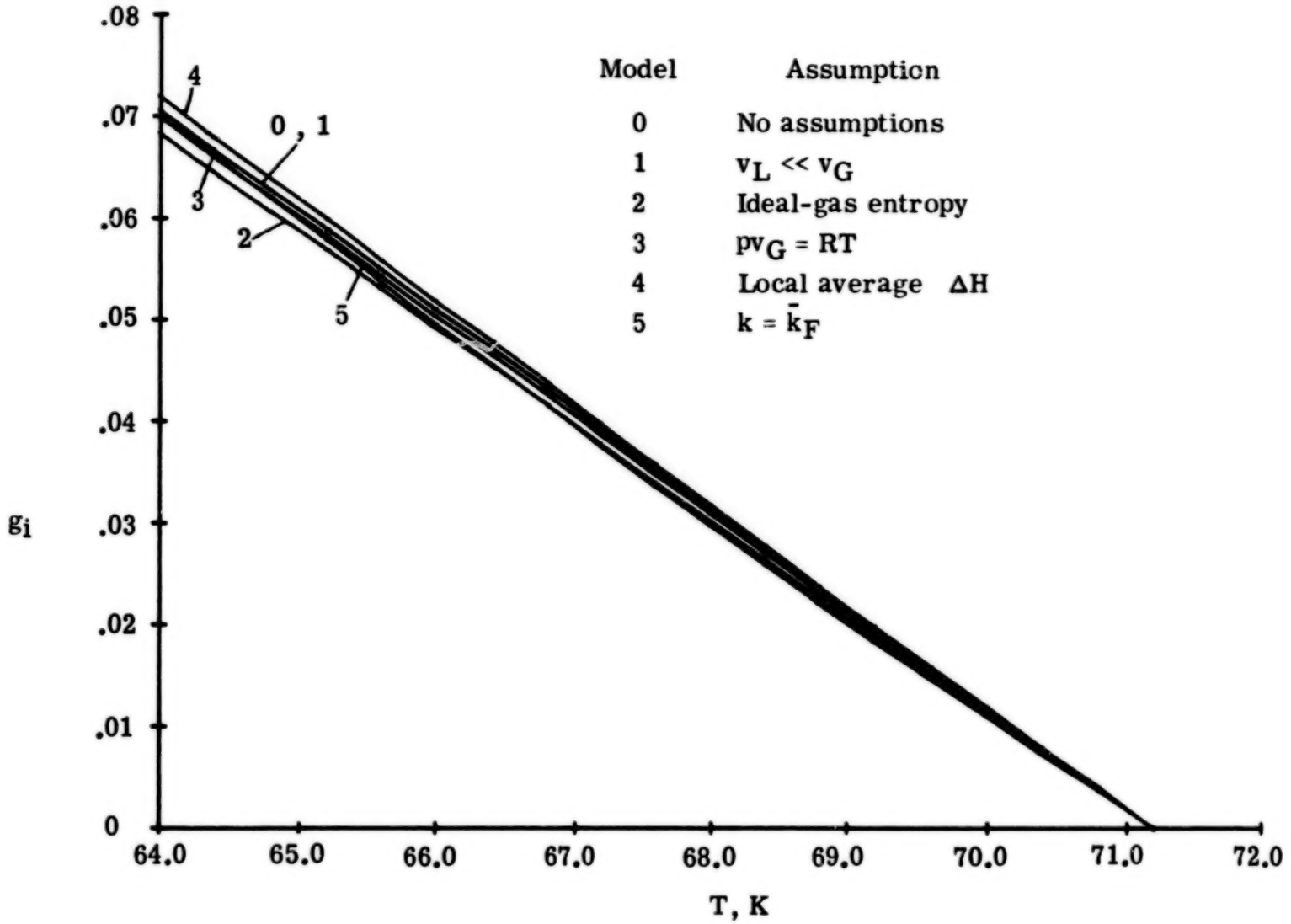

Figure 9.- Isentropic liquid mass fractions g_i for no-assumption and one-assumption models. T_C = 71.2 K; p_C = 0.45 atm; T_P = 64.0 K; p_P = 0.14 atm.

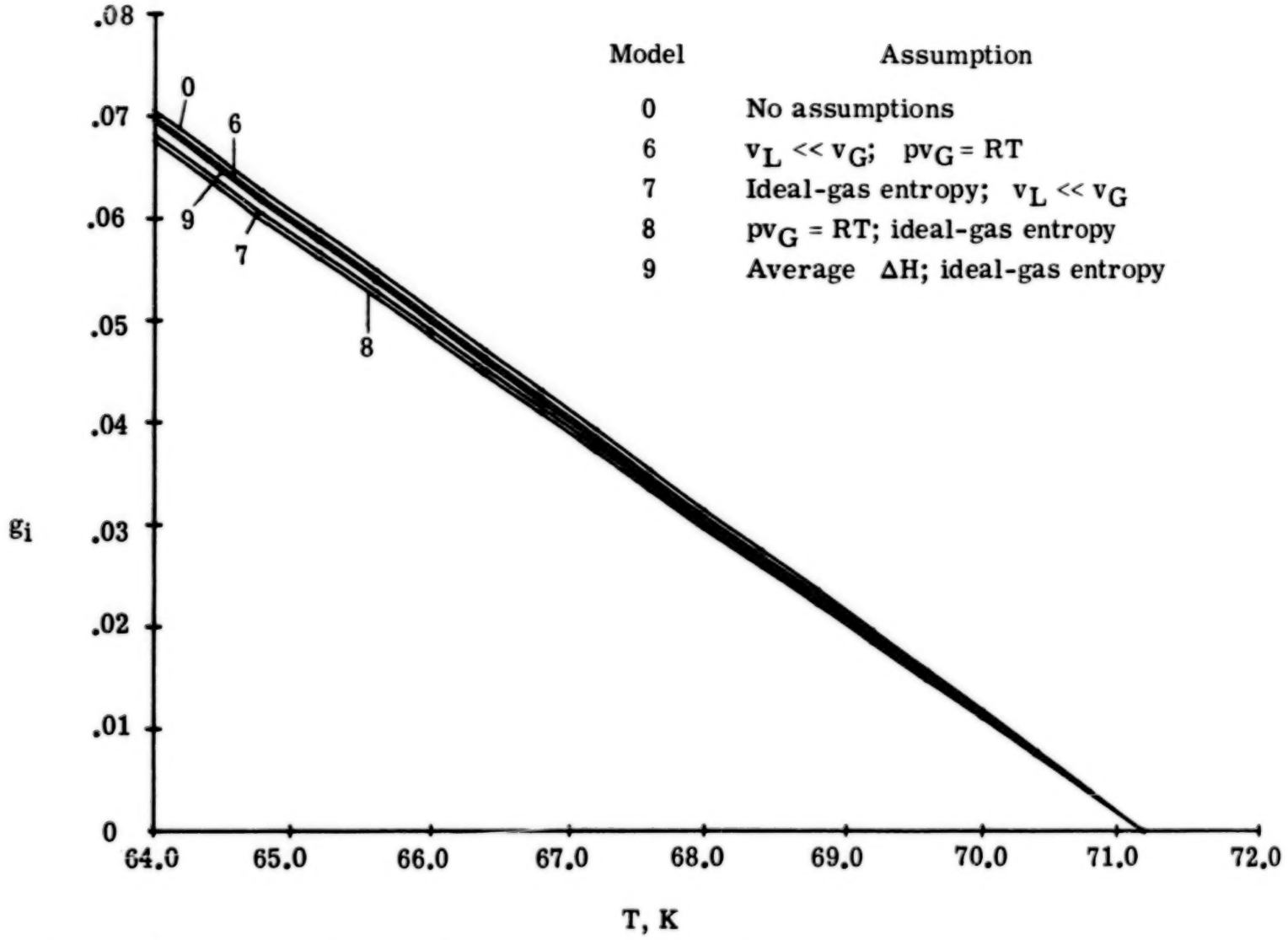

Figure 10.- Isentropic liquid mass fractions g_i for no-assumption and two-assumption models. T_C = 71.2 K; p_C = 0.45 atm; T_F = 64.0 K; p_F = 0.14 atm.

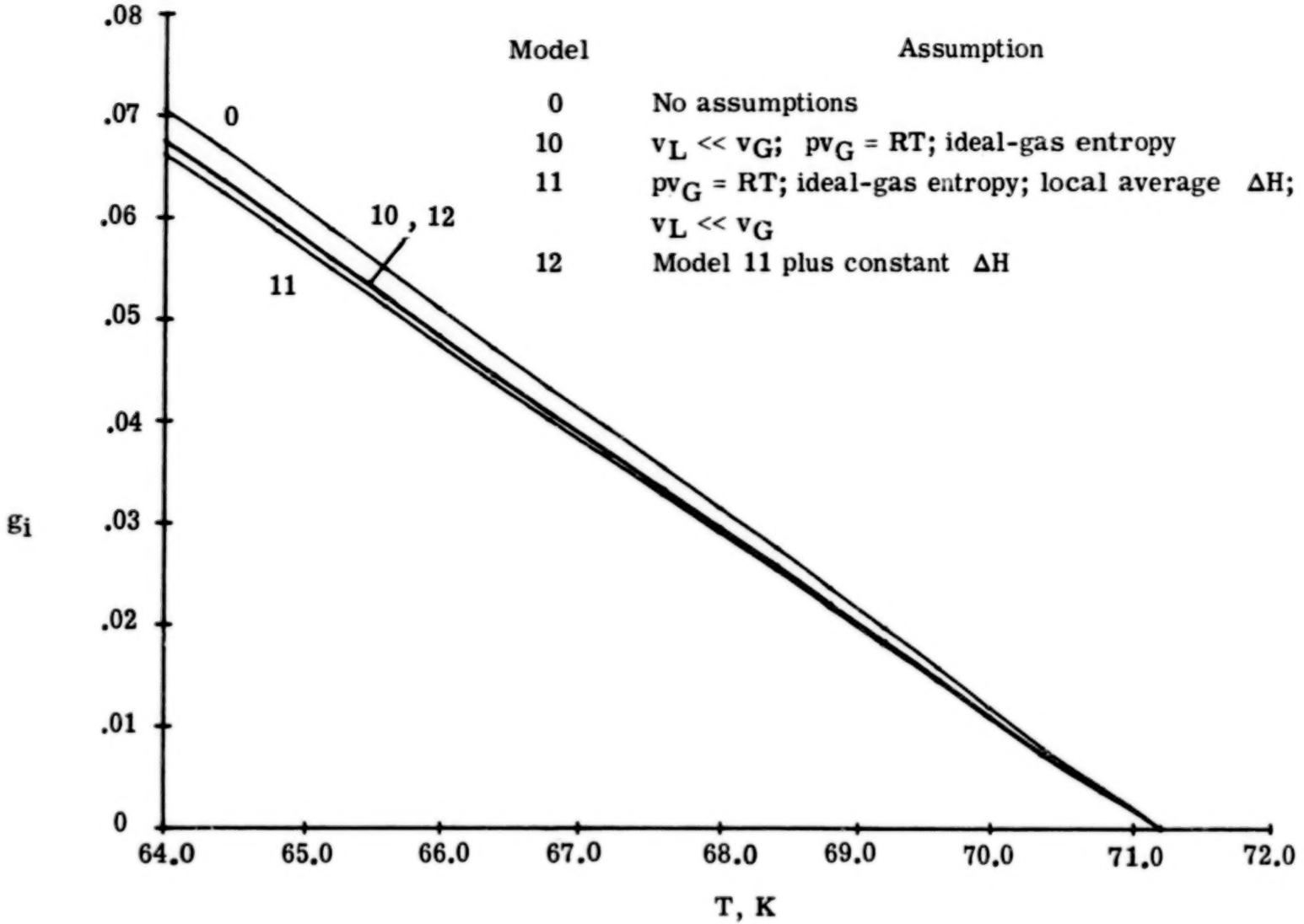

Figure 11.- Isentropic liquid mass fractions g_i for no-assumption and multiple-assumption models. T_C = 71.2 K; p_C = 0.45 atm; T_P = 64.0 K; p_P = 0.14 atm.

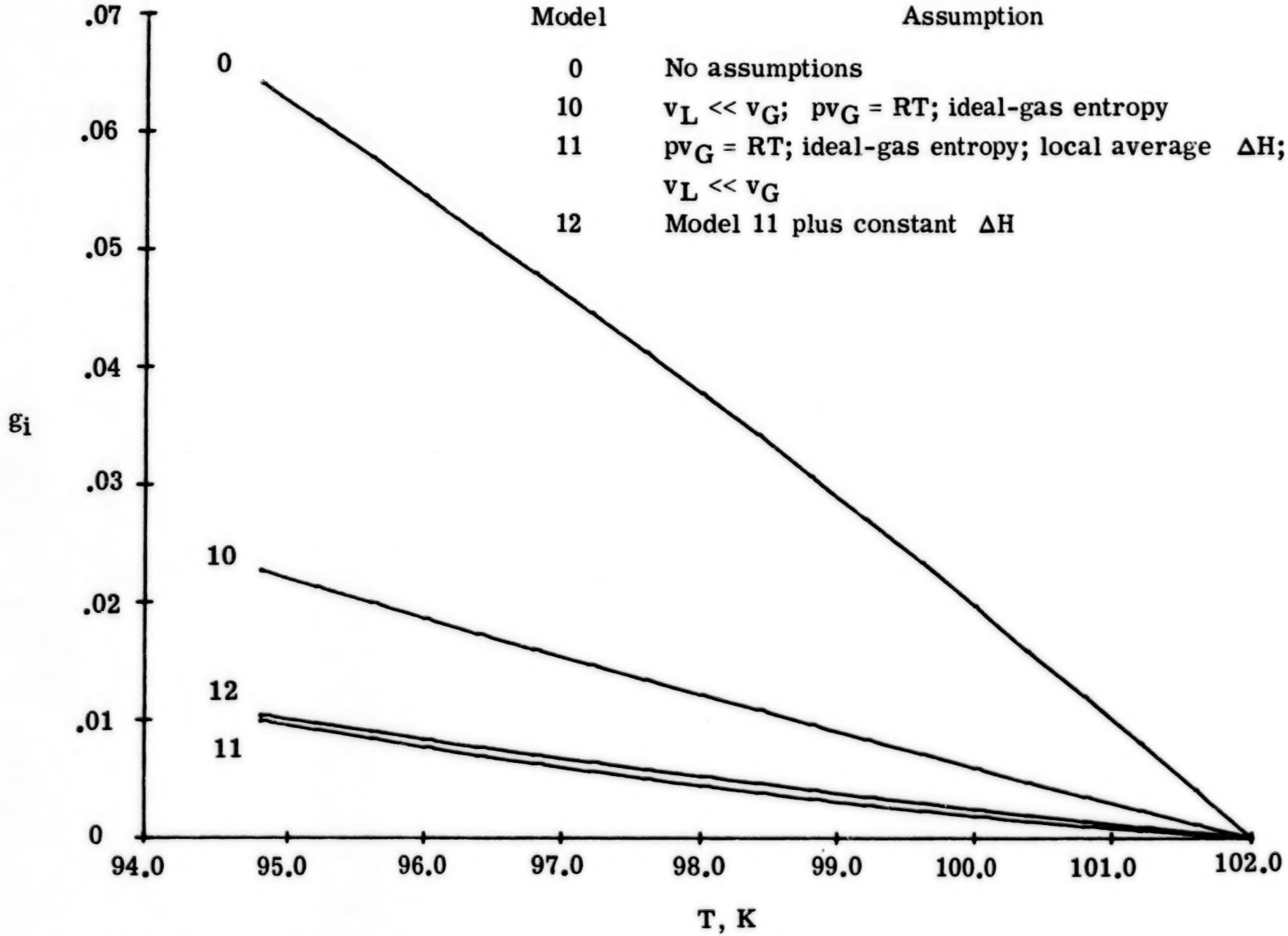

Figure 12.- Isentropic liquid mass fractions g_i for no-assumption and multiple-assumption models. Value of $C_{p,G}$, given by $[C_{p,G}(T_C) + C_{p,G}(T_F)]/2$, is taken to be 1418 J/kg·K. T_C = 102.0 K; p_C = 8.81 atm; T_F = 94.8 K; p_F = 5.26 atm.

1. Report No.	2. Government Accession No.	3. Recipient's Catalog No.
NASA TP-1682		

4. Title and Subtitle	5. Report Date
EFFECTS OF VARIOUS ASSUMPTIONS ON THE CALCULATED LIQUID FRACTION IN ISENTROPIC SATURATED EQUILIBRIUM EXPANSIONS	June 1980
	6. Performing Organization Code
7. Author(s)	8. Performing Organization Report No.
Joseph W. Bursik and Robert M. Hall	L-13437
	10. Work Unit No.
9. Performing Organization Name and Address	505-31-53-01
NASA Langley Research Center Hampton, VA 23665	11. Contract or Grant No.
	13. Type of Report and Period Covered
12. Sponsoring Agency Name and Address	Technical Paper
National Aeronautics and Space Administration Washington, DC 20546	14. Sponsoring Agency Code

15. Supplementary Notes

Joseph W. Bursik: Renssalaer Polytechnic Institute, Troy, New York.
Robert M. Hall: Langley Research Center.

16. Abstract

The saturated equilibrium expansion approximation for two-phase flow often involves ideal-gas and latent-heat assumptions to simplify the solution procedure. This approach is well documented by Wegener and Mack and works best at low pressures where deviations from ideal-gas behavior are small. A thermodynamic expression for liquid mass fraction that is decoupled from the equations of fluid mechanics is used in this paper to compare the effects of the various assumptions on nitrogen-gas saturated equilibrium expansion flow starting at 8.81 atm, 2.99 atm, and 0.45 atm, which are conditions representative of transonic cryogenic wind tunnels. For the highest-pressure case, the entire set of ideal-gas and latent-heat assumptions are shown to be in error by 62 percent for the values of heat capacity and latent heat used in this paper. An approximation of the exact, real-gas expression is also developed using a constant, two-phase isentropic expansion coefficient which results in an error of only 2 percent for the high-pressure case.

17. Key Words (Suggested by Author(s))	18. Distribution Statement
Saturated equilibrium expansion Nitrogen gas Cryogenic wind tunnel Real-gas analysis	Unclassified - Unlimited Subject Category 34

19. Security Classif. (of this report)	20. Security Classif. (of this page)	21. No. of Pages	22. Price*
Unclassified	Unclassified	30	$6.00

For sale by the National Technical Information Service, Springfield, Virginia 22161

NASA-Langley, 1980